Supporting Information for Development and Evaluation of Online Gas-Phase Chemistry in the Global Variable-Resolution Atmospheric Model iAMAS (v2.5.1): Resolution-Dependent Surface Ozone over North China

Zihan Xia [1], Chun Zhao [1,2*], Chen Jin [1], Xin Qu [1], Zining Yang [1], Ziyu Zhang [1], Qike Yang [1], Jun Gu [3], Gudongze Li [1], Jiawang Feng [1], Shen Du [1], Jane Liu [4]

[1]School of Earth and Space Sciences/CMA-USTC Laboratory of Fengyun Remote Sensing/State Key Laboratory of Fire Science/Institute of Advanced Interdisciplinary Research on High-Performance Computing Systems and Software, University of Science and Technology of China, Hefei, China

[2]Laoshan Laboratory, Qingdao, China

[3]Department of Atmospheric and Oceanic Sciences / Institute of Atmospheric Sciences, Fudan University, Shanghai, China

[4]Department of Geography and Planning, University of Toronto, Toronto, Canada

Correspondence to: Chun Zhao (chunzhao@ustc.edu.cn)

Contents of this file

Text S1 and Figures S1–S10

Text S1. WRF-Chem Reference Simulation

WRF-Chem is one of the most widely used regional chemistry-transport models and has been extensively evaluated against observations over East Asia and globally (Grell et al., 2005; Fast et al., 2006). A WRF-Chem simulation is included here to provide qualitative context for assessing whether iAMAS performance falls within a reasonable range relative to an established community model operating under broadly comparable conditions.

The WRF-Chem simulation was conducted at 0.5° horizontal resolution over a near-global domain (65.25°S–74.25°N, 179.75°W–179.75°E) for July 2019, using the same block-cycling ERA5 meteorological reinitialization protocol as iAMAS. The physical and chemical parameterization suite is closely matched to the iAMAS configuration, including the SAPRC-99 gas-phase mechanism, the YSU planetary boundary layer scheme, the Thompson microphysics scheme, and the RRTMG radiation scheme. The principal differences between the two configurations are as follows: the ozone chemical initial conditions in WRF-Chem are derived from MOZART-4 reanalysis output rather than the TOST-v2 ozonesonde climatology used in iAMAS; the HTAP anthropogenic and FINN fire emission inventories are of slightly different versions; the dynamical time step is 120 s in WRF-Chem compared to 300 s in iAMAS U60km, reflecting their respective resolution requirements; and the model top is set to 50 hPa in WRF-Chem compared to approximately 30 km in iAMAS. Additionally, as a limited-area model, WRF-Chem requires prescribed lateral boundary conditions derived from global reanalysis, which introduces chemical boundary uncertainties that are absent in the global iAMAS framework. Given these configurational differences, the WRF-Chem results presented in Figures S3–S7 are intended as a qualitative reference only and should not be interpreted as a direct quantitative benchmark for iAMAS performance.

Figures S1–S10

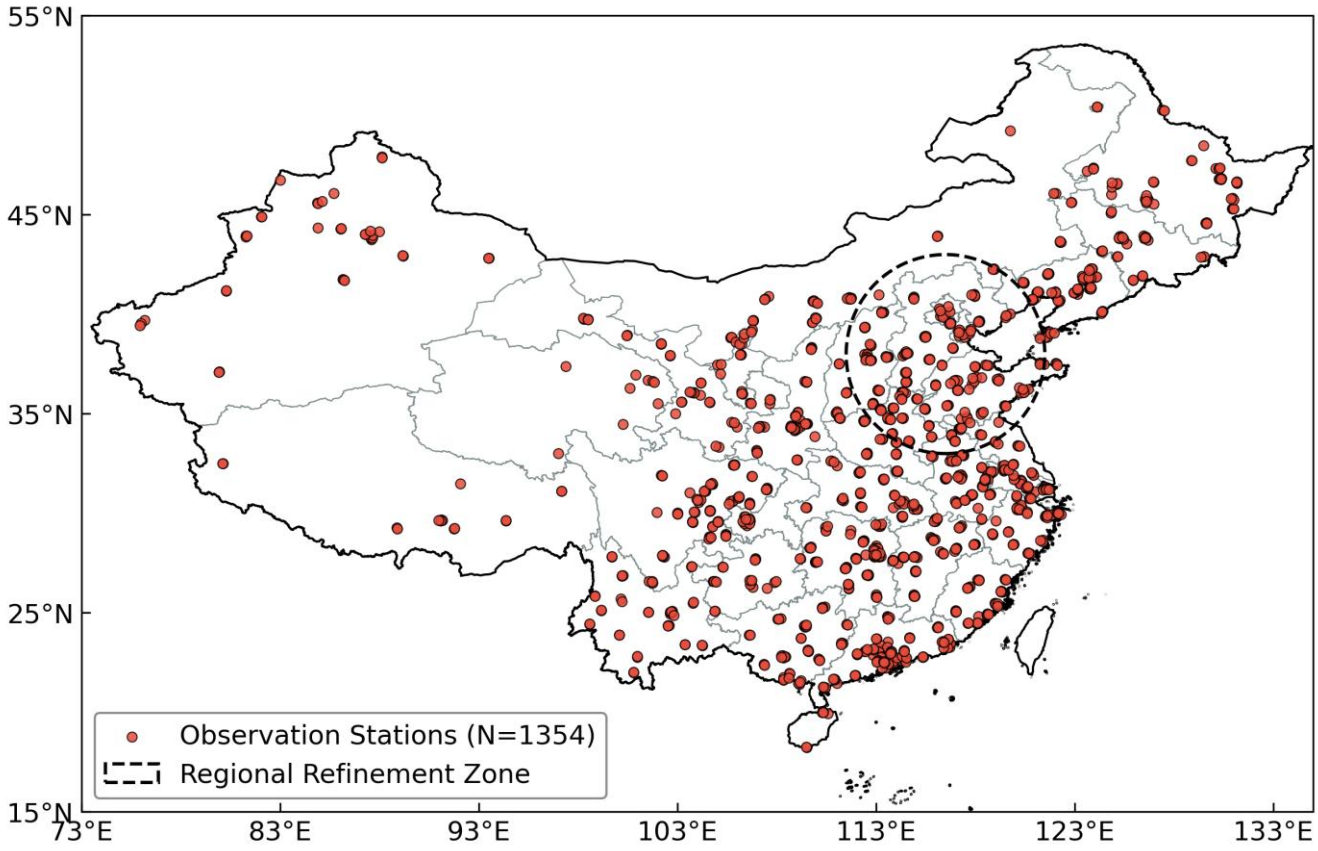

Figure S1. National spatial distribution of air quality monitoring stations in China. Red circles denote the locations of all valid ground observation stations (N = 1354) used in this study. The black dashed circle marks the regional refinement zone (centered at 116.5°E, 38.0°N with a 5.0° radius) covering the Beijing-Tianjin-Hebei area and parts of the Taihang Mountains.

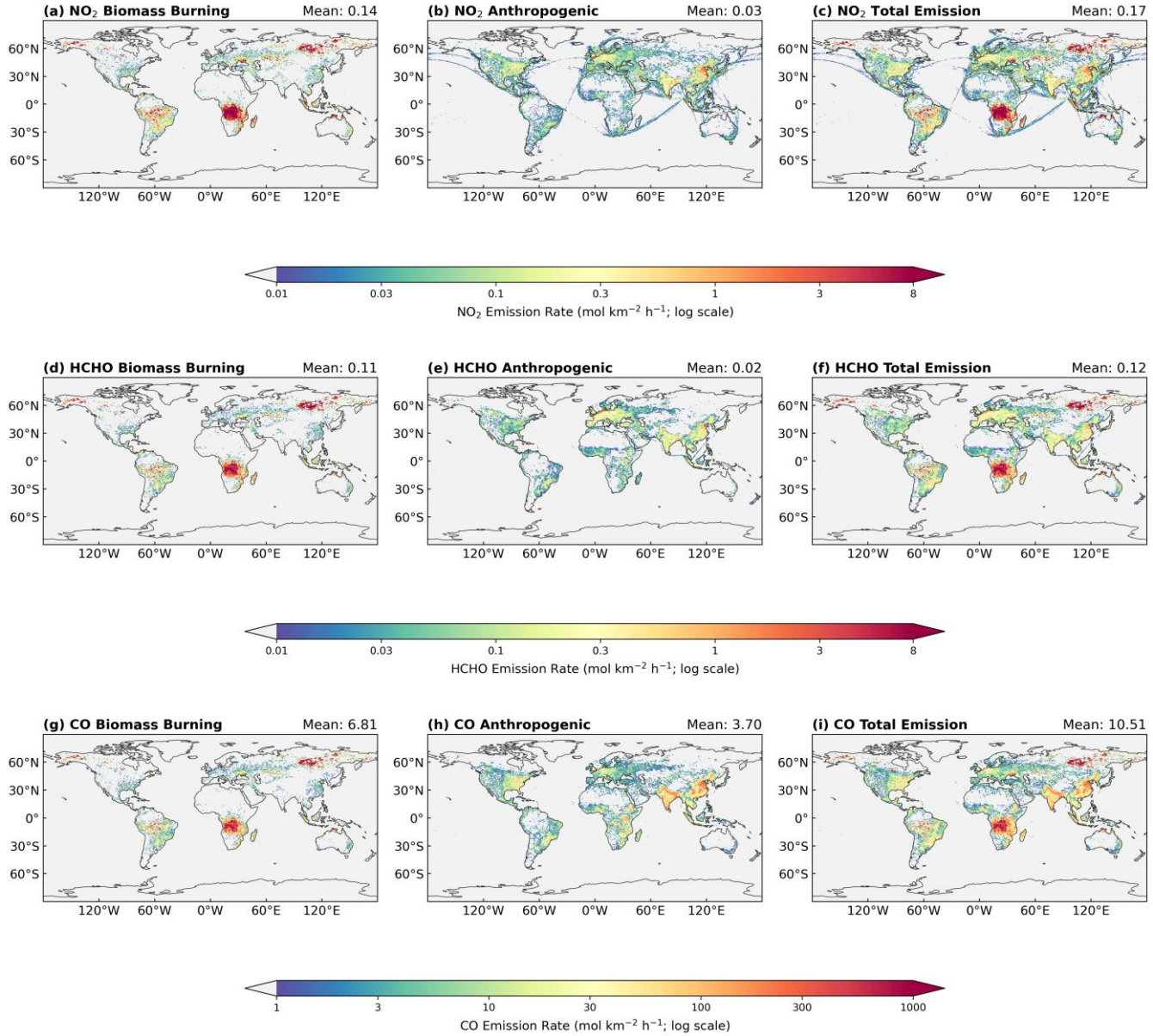

Figure S2. Global distributions of monthly mean biomass-burning, anthropogenic, and total emissions of NO_2, HCHO, and CO. Colours show emission rates (mol km^{-2} h^{-1}) using a logarithmic scale for each species row; the same scale is applied to all three source categories within a row. Mean values are reported above each panel.

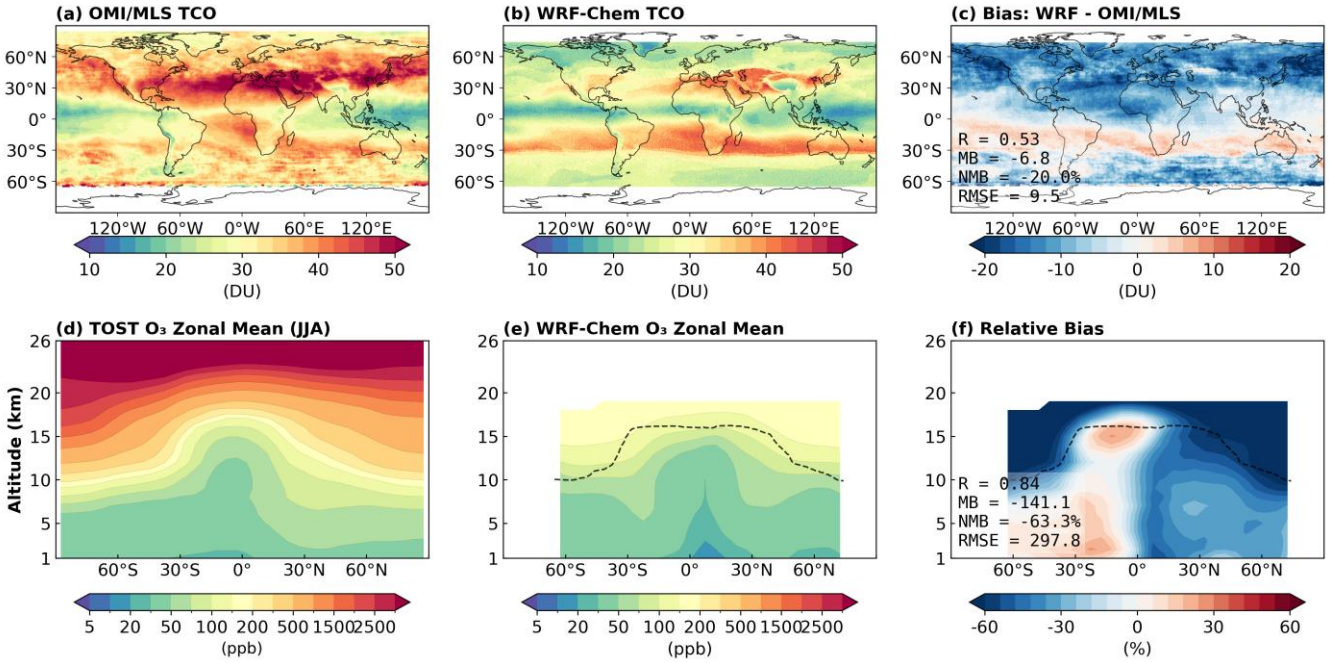

Figure S3. Same as Figure 3, but for the WRF-Chem reference simulation at 0.5° horizontal resolution. Global statistics for TCO (panels a–c): R = 0.53, MB = −6.8 DU, NMB = −20.0%, RMSE = 9.5 DU. Global statistics for zonal-mean ozone (panels d–f): R = 0.84, MB = −141.1 ppb, NMB = −63.3%, RMSE = 297.8 ppb. Note that the WRF-Chem domain does not extend to high latitudes, resulting in the data gap visible in the figure.

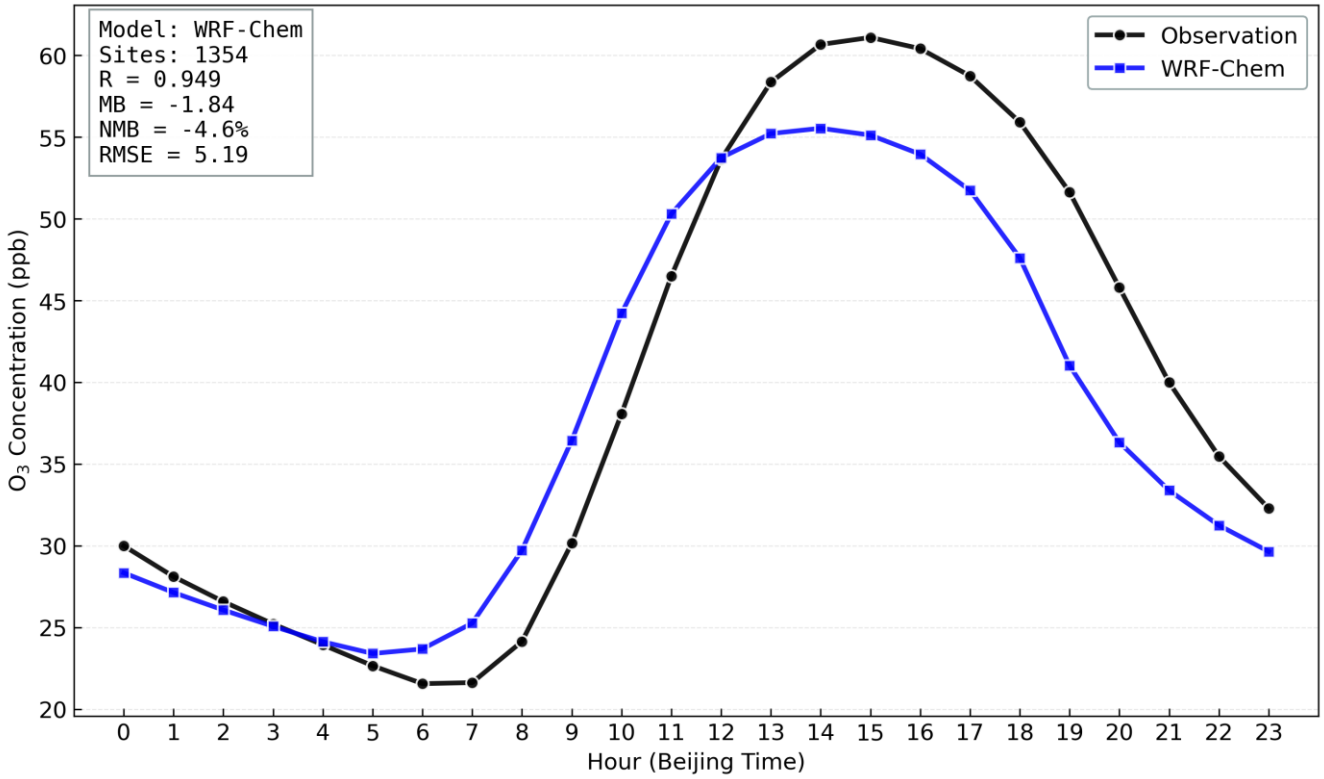

Figure S4. Same as Figure 4, but for the WRF-Chem reference simulation. Statistics: R = 0.949, MB = −1.84 ppb, NMB = −4.6%, RMSE = 5.19 ppb.

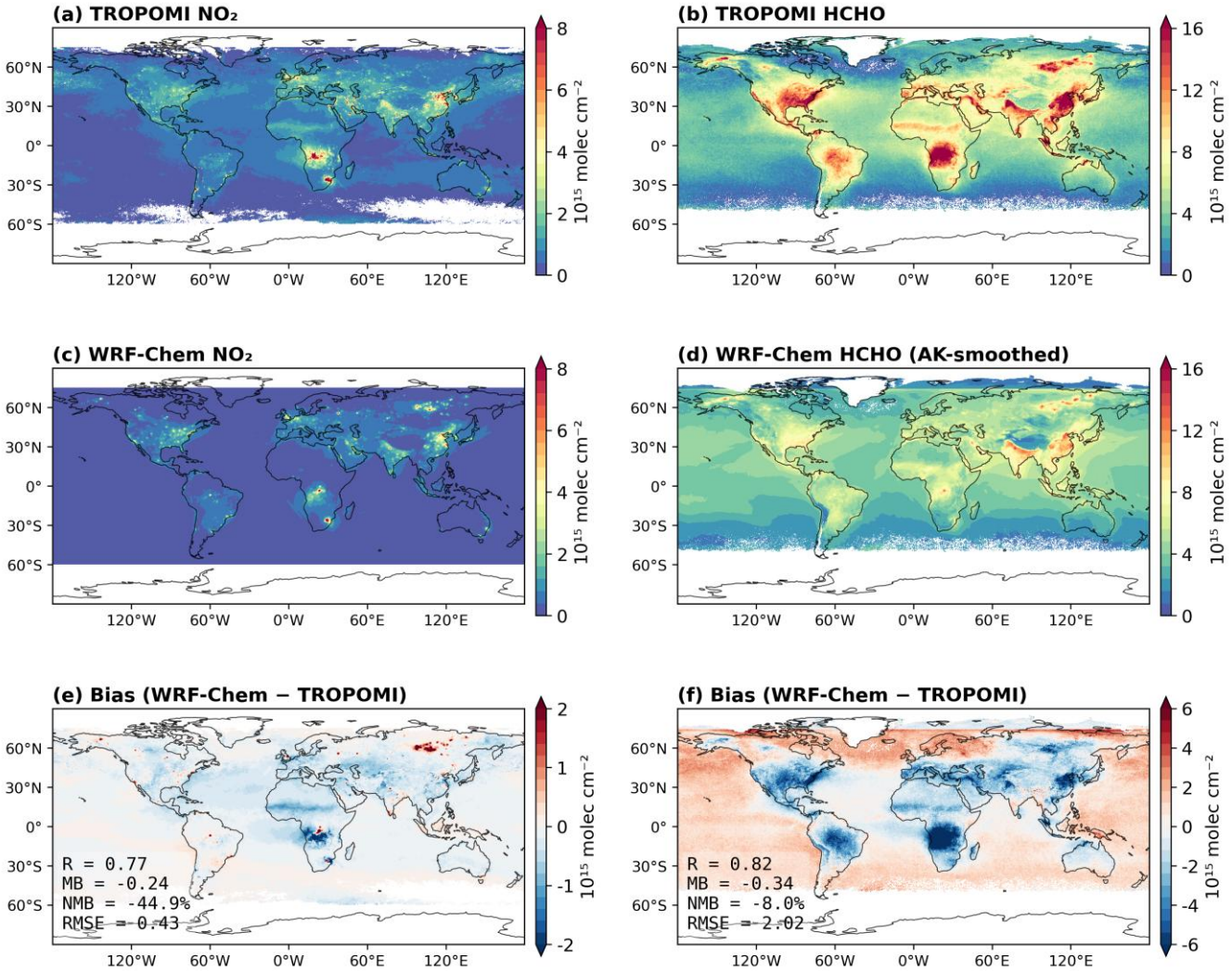

Figure S5. Same as Figure 5, but for the WRF-Chem reference simulation. NO_2 statistics (panel e): R = 0.77, MB = −0.24 × 10^{15} molecules cm^{-2}, NMB = −44.9%, RMSE = 0.43 × 10^{15} molecules cm^{-2}. HCHO statistics (panel f): R = 0.82, MB = −0.34 × 10^{15} molecules cm^{-2}, NMB = −8.0%, RMSE = 2.02 × 10^{15} molecules cm^{-2}.

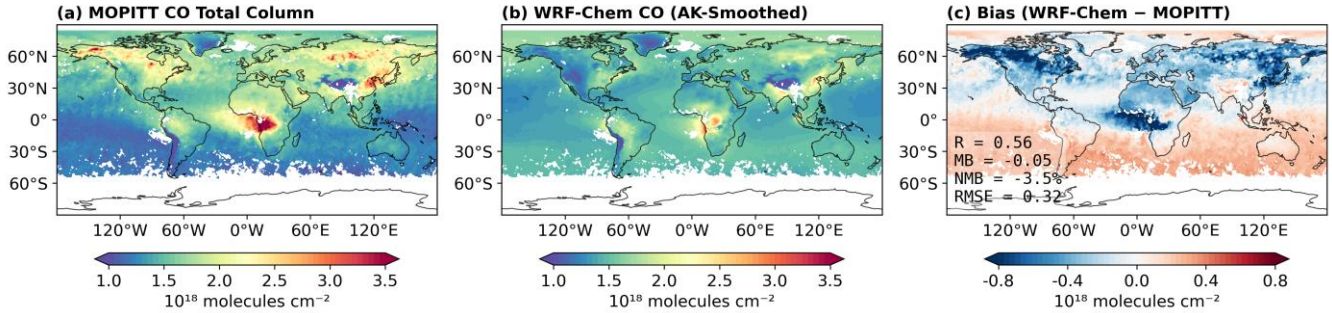

Figure S6. Same as Figure 6, but for the WRF-Chem reference simulation. Global statistics: R = 0.56, MB = −0.05 × 10^{18} molecules cm^{-2}, NMB = −3.5%, RMSE = 0.32 × 10^{18} molecules cm^{-2}.

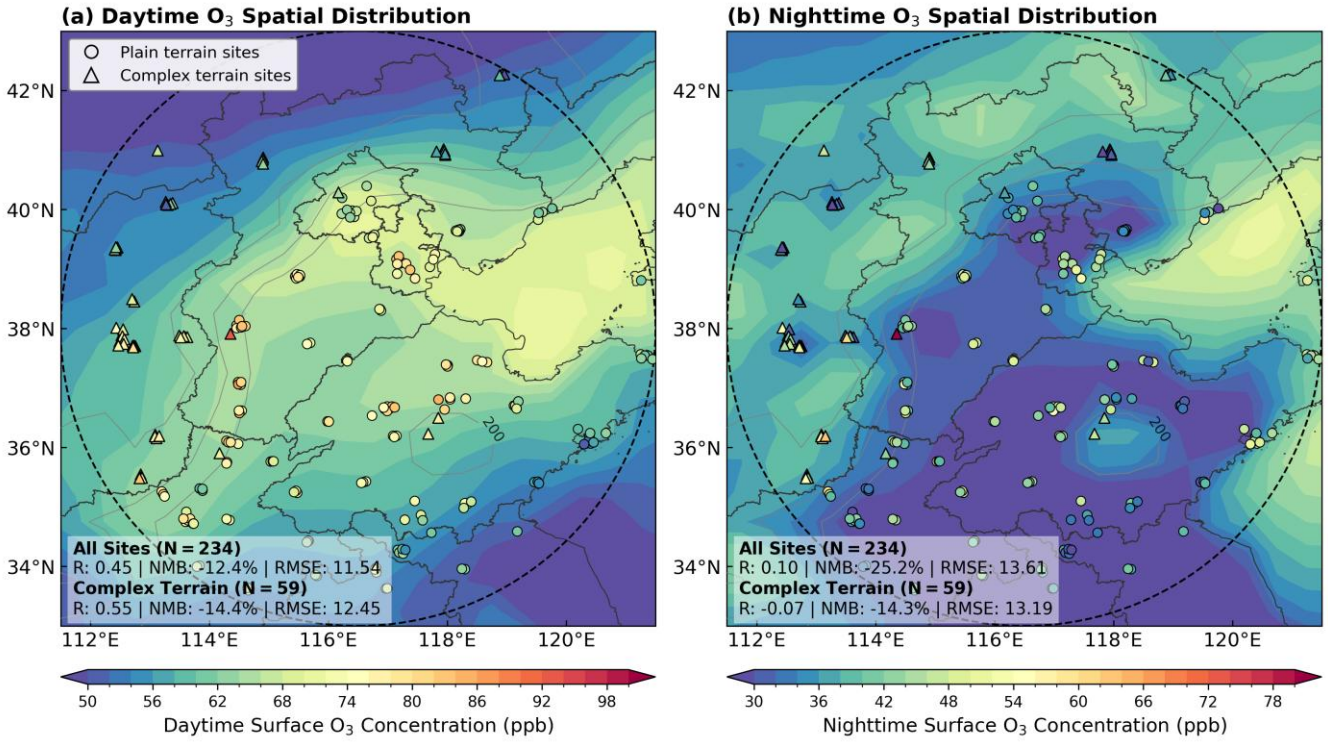

Figure S7. Evaluation of WRF-Chem (0.5° resolution) surface O_3 over the North China refinement zone for July 2019. (a) Daytime (08:00–19:00 BJT) and (b) nighttime (20:00–07:00 BJT) spatial distributions of WRF-Chem simulated surface O_3 (background shading) with observed CNEMC station concentrations overlaid. Statistical metrics (R, NMB, RMSE) are shown separately for all sites and complex-terrain sites.

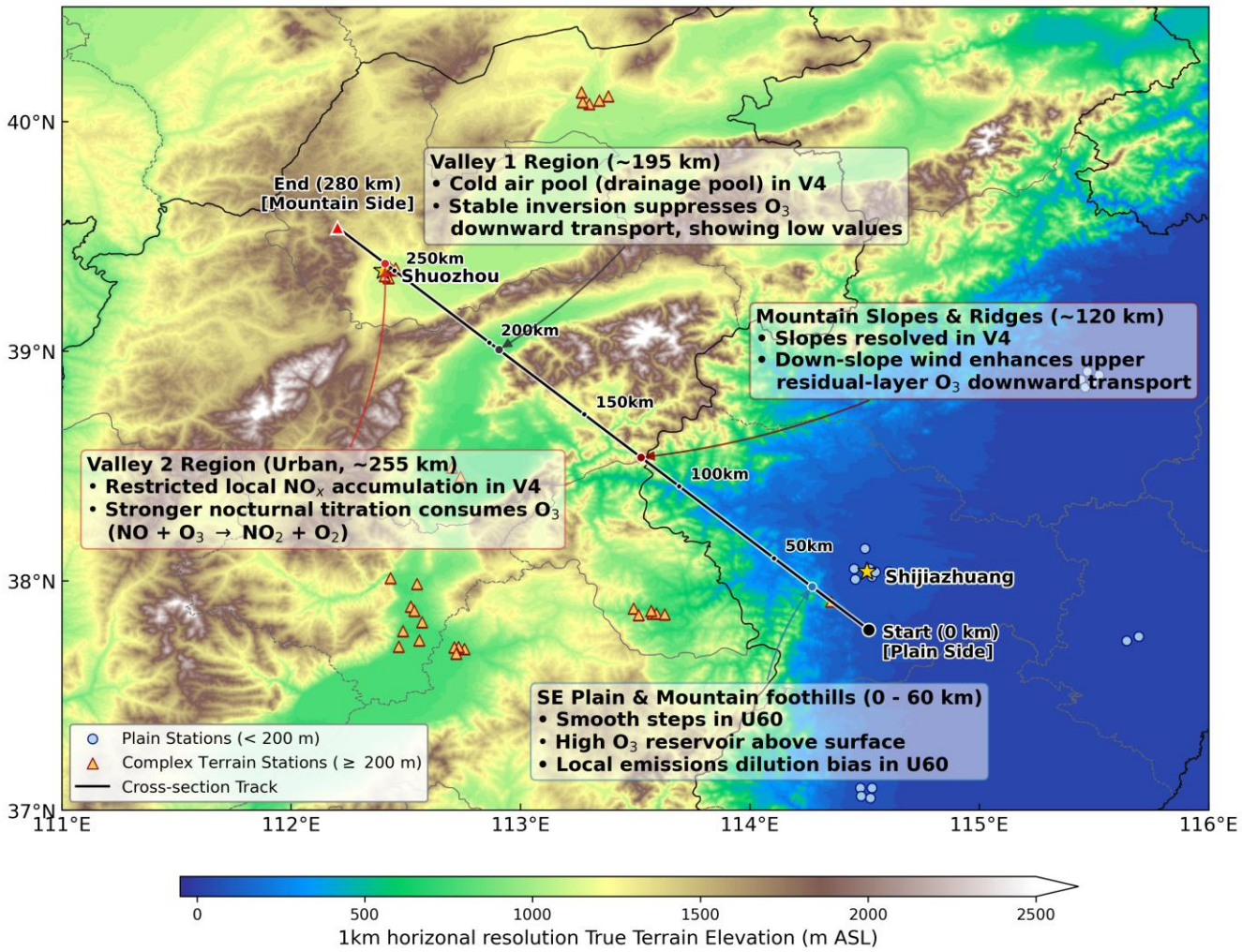

Figure S8. Topographic schematic of the cross-section transect used in Figure 8. Background shading shows approximately 1 km horizontal-resolution reference terrain elevation (m ASL). The black line marks the SE–NW transect track, with distance markers at 50 km intervals. Annotated boxes indicate key terrain zones along the transect: SE plain and mountain foothills (0–60 km), mountain slopes and ridges (~120 km), Valley 1 (~195 km), and urban Valley 2 (~250 km, Shuozhou). Orange triangles denote complex terrain monitoring sites; blue circles denote plain sites.

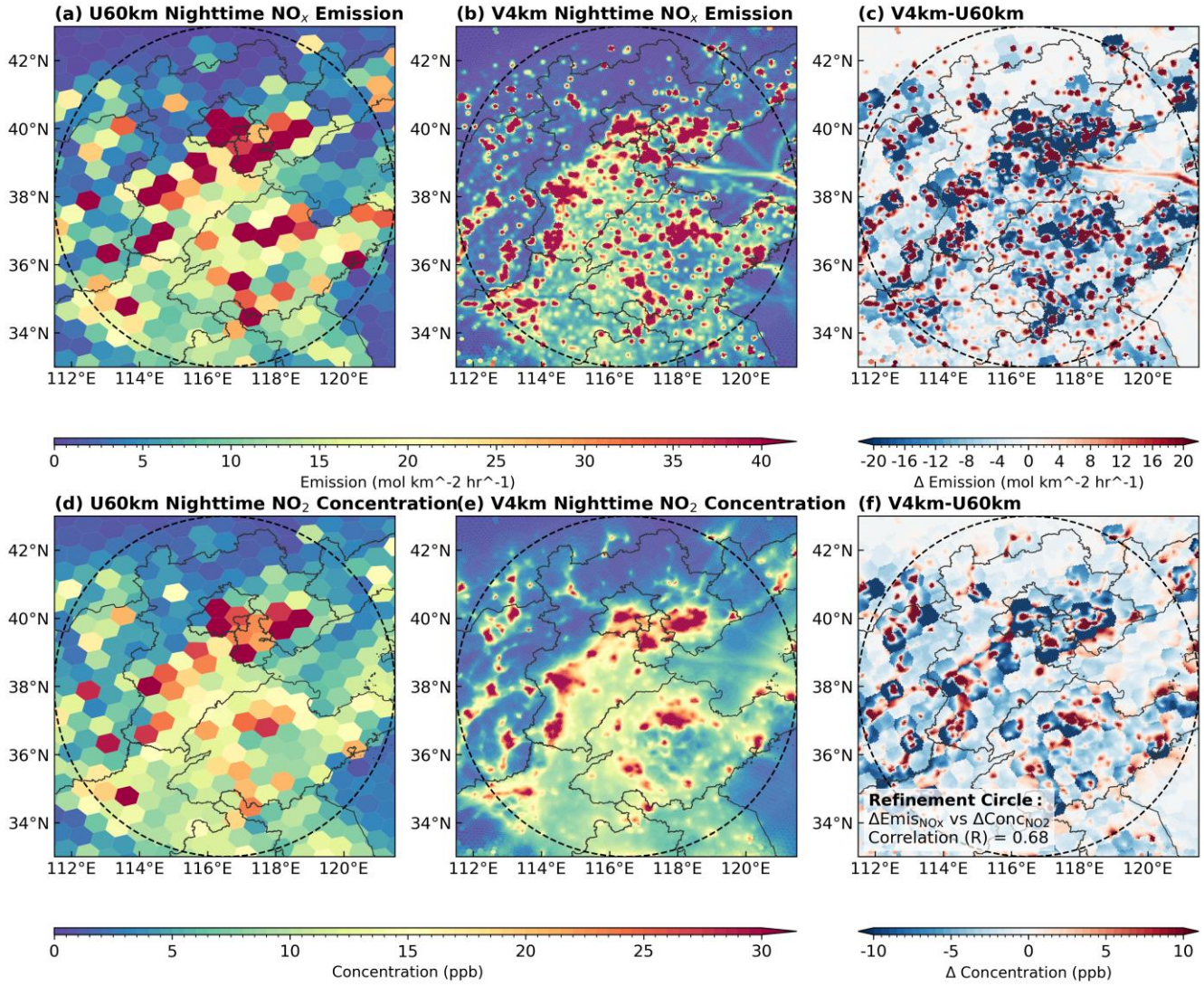

Figure S9. Nighttime (20:00–07:00 BJT) surface NO_x emission rates and NO_2 concentrations over the North China refinement zone for July 2019. (a, b) U60km and V4km NO_x emission rates (mol km^{-2} h^{-1}); (c) V4km − U60km NO_x emission difference; (d, e) U60km and V4km surface NO_2 concentrations (ppb); (f) V4km − U60km NO_2 concentration difference. The spatial correlation between ΔNO_x emission and ΔNO_2 concentration within the refinement zone is annotated in panel (f).

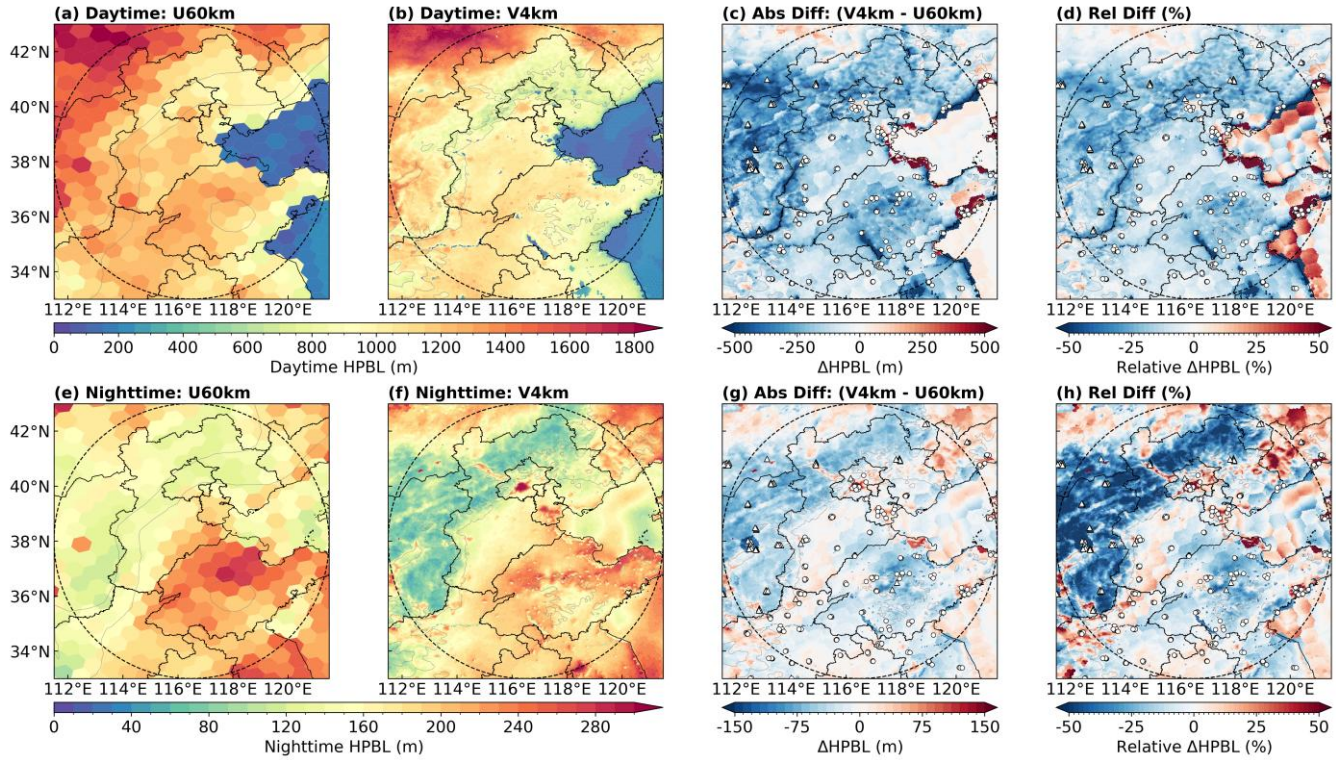

Figure S10. Daytime (08:00–19:00 BJT) and nighttime (20:00–07:00 BJT) planetary boundary layer height (PBLH) spatial distributions and resolution impacts over the North China refinement zone for July 2019. (a, b) Daytime U60km and V4km PBLH (m); (c) daytime absolute difference ΔPBLH (m); (d) daytime relative difference (%); (e, f) nighttime U60km and V4km PBLH; (g) nighttime absolute ΔPBLH; (h) nighttime relative difference (%). Note that color scale ranges differ between daytime and nighttime panels. Plain terrain and complex terrain monitoring sites are overlaid as circles and triangles, respectively.